Evolutionary and Molecular Facts Link the WWC Protein Family to Hippo Signaling

Dirk Oliver Wennmann,[1] Jürgen Schmitz,[2] Michael C. Wehr,[3] Michael P. Krahn,[4] Nora Koschmal,[4] Sascha Gromnitza,[1] Ulf Schulze,[1] Thomas Weide,[1] Anil Chekuri,[1] Boris V. Skryabin,[2,5] Volker Gerke,[6] Hermann Pavenstädt,[1] Kerstin Duning,[†,1] and Joachim Kremerskothen[*,†,1]

[1]Internal Medicine D, Department of Nephrology, Hypertension and Rheumatology, University Hospital Muenster, Muenster, Germany

[2]Institute of Experimental Pathology, ZMBE, University of Muenster, Muenster, Germany

[3]Department of Psychiatry, Molecular Neurobiology, Ludwig Maximilians University, Munich, Germany

[4]Institute for Molecular and Cellular Anatomy, University of Regensburg, Regensburg, Germany

[5]IZKF, University Hospital Muenster, Muenster, Germany

[6]Institute of Medical Biochemistry, ZMBE, University of Muenster, Muenster, Germany

[†]These authors contributed equally to this work.

***Corresponding author:** E-mail: kremers@uni-muenster.de.

Associate editor: Stuart Newfeld

Abstract

The scaffolding protein KIBRA (also called WWC1) is involved in the regulation of important intracellular transport processes and the establishment of cell polarity. Furthermore, KIBRA/WWC1 is an upstream regulator of the Hippo signaling pathway that controls cell proliferation and organ size in animals. KIBRA/WWC1 represents only one member of the WWC protein family that also includes the highly similar proteins WWC2 and WWC3. Although the function of KIBRA/WWC1 was studied intensively in cells and animal models, the importance of WWC2 and WWC3 was not yet elucidated. Here, we describe evolutionary, molecular, and functional aspects of the WWC family. We show that the WWC genes arose in the ancestor of bilateral animals (clades such as insects and vertebrates) from a single founder gene most similar to the present KIBRA/WWC1-like sequence of *Drosophila*. This situation was still maintained until the common ancestor of lancelet and vertebrates. In fish, a progenitor-like sequence of mammalian KIBRA/WWC1 and WWC2 is expressed together with WWC3. Finally, in all tetrapods, the three family members, KIBRA/WWC1, WWC2, and WWC3, are found, except for a large genomic deletion including WWC3 in *Mus musculus*. At the molecular level, the highly conserved WWC proteins share a similar primary structure, the ability to form homo- and heterodimers and the interaction with a common set of binding proteins. Furthermore, all WWC proteins negatively regulate cell proliferation and organ growth due to a suppression of the transcriptional activity of YAP, the major effector of the Hippo pathway.

Key words: **KIBRA, WWC family, Hippo pathway, LATS kinase, YAP, organ size.**

Article

Introduction

Central cellular mechanisms are regulated by complex and dynamic protein–protein networks. Scaffolding proteins are crucial for these processes as they recruit functional protein complexes to distinct locations within the cytoplasm, to the nucleus or to cell membranes. The scaffold protein KIBRA (for KIdney and BRAin, also called WWC1 for WW-and-C2-domain-containing-protein-1; Kremerskothen et al. 2003) is involved in cellular transport processes crucial for cell migration (Rosse et al. 2009), cell polarity (Traer et al. 2007; Duning et al. 2008), synaptic signaling (Kremerskothen et al. 2003; Makuch et al. 2011), and higher brain functions (Schneider et al. 2010; Duning et al. 2013). More specifically, KIBRA/WWC1 regulates exocytosis of the transferrin receptor through an interaction with Dynein Light Chain 1 (DLC1) and Sorting Nexin 4 (SNX4) (Traer et al. 2007). In renal podocytes, KIBRA/WWC1 has an impact on targeted cell migration and links polarity complexes to the cytoskeleton (Duning et al. 2008). In neurons, KIBRA/WWC1 impairs recycling of AMPA receptors to postsynaptic membranes via an association with protein interacting with C kinase 1 (PICK1) (Makuch et al. 2011). KIBRA/WWC1 also influences the size of the apical membrane through a localized interaction and inhibition of the atypical protein kinase C (aPKC) (Yoshihama et al. 2011).

Recent studies in *Drosophila melanogaster* and mammalian cells identified KIBRA/WWC1 as a regulatory element of the Hippo pathway, which has been linked to various cellular processes including growth control, cellular polarity, contact inhibition, and mechanotransduction (reviewed in Yu and Guan 2013). The highly conserved Hippo pathway integrates extracellular signals via G protein-coupled receptors, Wnt, and TGF-β signaling and downstream regulators (Varelas et al. 2008a, 2010; Yu, Zhao et al. 2012). At its core lies a kinase cassette formed of the mammalian Ste20-like kinases 1 and 2, MST1/2 (*Drosophila* Hippo) and the large tumor

suppressor 1 and 2 kinases, LATS1/2 (*Drosophila* Warts). The kinase cassette controls the activity of the co-transcriptional activators Yes-associated-protein (YAP) and its family member transcriptional coactivator with PDZ-binding Motif (TAZ) (*Drosophila* Yorkie), which are the key output regulators of the Hippo pathway (Yin and Zhang 2011; Yu, Mo et al. 2012; Harvey et al. 2013). Although activation of the Hippo pathway leads to phosphorylation and cytosolic retention of YAP/TAZ, an inhibition of Hippo signaling decreases YAP/TAZ phosphorylation levels to promote their nuclear import (Dong et al. 2007; Zhao et al. 2010). In association with the TEAD family transcription factors, nuclear YAP/TAZ facilitates transcription of target genes to promote cell proliferation and organ growth (Zhao et al. 2009, 2011; Yin and Zhang 2011). Through an interaction with several upstream Hippo pathway components including the neurofibromatosis protein 2 (NF2, Merlin in *Drosophila*), the protein tyrosine phosphatase nonreceptor type 14 (PTPN14, Pez in *Drosophila*), and LATS1/2, KIBRA/WWC1 activates the phosphorylation of YAP to inhibit cell proliferation (Genevet et al. 2010; Yu et al. 2010; Jukam and Desplan 2011; Xiao, Chen, Ji, Dong, et al. 2011; Poernbacher et al. 2012). Therefore, KIBRA/WWC1 is supposed to play a role as a tumor suppressor regulating organ growth.

In contrast to invertebrates that express only one KIBRA/WWC1-like protein, the genomes of mammals encode a whole WWC protein family that includes KIBRA/WWC1 and the highly similar, but so far not characterized proteins WWC2 and WWC3 (Yoshihama et al. 2012). To further address their functional roles, we performed a detailed evolutionary, molecular, and functional analysis of the individual WWC proteins. We suggest that evolution of the WWC proteins arose from a single KIBRA/WWC1-like sequence in the bilateral ancestor of animals. In fish, a proposed common progenitor of the later KIBRA/WWC1 and WWC2 (WWC1/WWC2) as well as WWC3 are expressed. Finally, mammalian genomes (excluding *Mus musculus*) contain genes encoding all three WWC proteins (KIBRA/WWC1, WWC2, and WWC3).

An expression analysis revealed the WWC genes to be differentially regulated in a tissue-specific manner. In addition, the WWC proteins are able to form homo- and heterodimers and share a binding activity toward DLC1, aPKC, and LATS kinases. Importantly, the function as a negative regulator of YAP transcriptional activity, Hippo signaling, and cell proliferation is evolutionary conserved from the KIBRA progenitor in flies to all three WWC proteins expressed in mammals.

Results

Structural Characteristics of the WWC Proteins

To address the structural characteristics of the individual WWC proteins, we first cloned the full-length open-reading frame (ORF) for human WWC3 as former database entries represented only an amino terminal-truncated version of this protein (see Materials and Methods and supplementary fig. S1, Supplementary Material online). A subsequent alignment of the amino acid sequences from human KIBRA/WWC1, WWC2, and WWC3 (supplementary fig. S2, Supplementary Material online) revealed that KIBRA/WWC1 has a total sequence identity of 49% with WWC2 and of 40% with WWC3. WWC2 and WWC3 share a sequence identity of 43%. All WWC proteins have two amino terminal WW domains that mediate binding to target proteins harboring L/PPxY motifs and an internal C2 domain for membrane association (fig. 1 and supplementary fig. S3, Supplementary Material online). At the carboxy terminus, all WWC proteins display a common binding site for aPKC (aPKC bs) and share a class III PDZ-interaction motif (ADDV). KIBRA/WWC1 contains a specific, glutamic acid-rich region adjacent to the C2 domain. In contrast, WWC3 displays an arginine- and proline-rich sequence stretch that precedes the two WW domains (fig. 1 and supplementary fig. S3, Supplementary Material online).

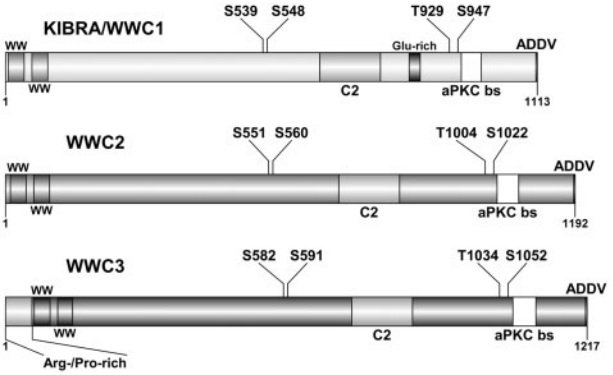

Fig. 1. Domain structure of the three human WWC proteins. Human KIBRA/WWC1 (1,113 aa), WWC2 (1,192 aa), and WWC3 (1,217 aa) share a common protein architecture with two amino terminal WW domains, an internal C2 domain, a binding site for aPKC (aPKC bs), and a carboxy terminal interaction motif (ADDV) for PDZ domain-containing proteins. A carboxy terminal glutamic (Glu)-rich sequence is unique for KIBRA/WWC1 and an amino terminal arginine- and proline-rich (Arg-/Pro-rich) domain is only present in WWC3. Important phosphorylation sites that are found in all WWC proteins are indicated.

KIBRA/WWC1 is a substrate of different kinases such as Aurora A/B (phosphorylation site serine 539 (S539); Xiao, Chen, Ji, Volle, et al. 2011), the extracellular signal-regulated kinase (ERK; S548), and the 90-kDa ribosomal S6 kinase (RSK; T929 and S947) and posttranslational phosphorylation of KIBRA/WWC1 sites was found to control its cellular activity (Yang et al. 2014). Interestingly, homologs of the KIBRA/WWC1 phosphorylation motifs are also present in WWC2 and WWC3, pointing to a common posttranslational regulatory mechanism of the WWC protein activity (fig. 1).

Phylogenesis of the WWC Protein Family

Genome annotation data provide the first glimpse into the evolution of the KIBRA/WWC1 and the KIBRA-like genes WWC2 and WWC3 (fig. 2A). Using the presence or absence of WWC sequences in different taxonomic groups, we derived an evolutionary scenario showing invertebrates (e.g., *Drosophila*) with a single WWC-like form, and placed this form at the base of the WWC evolutionary tree (fig. 2A).

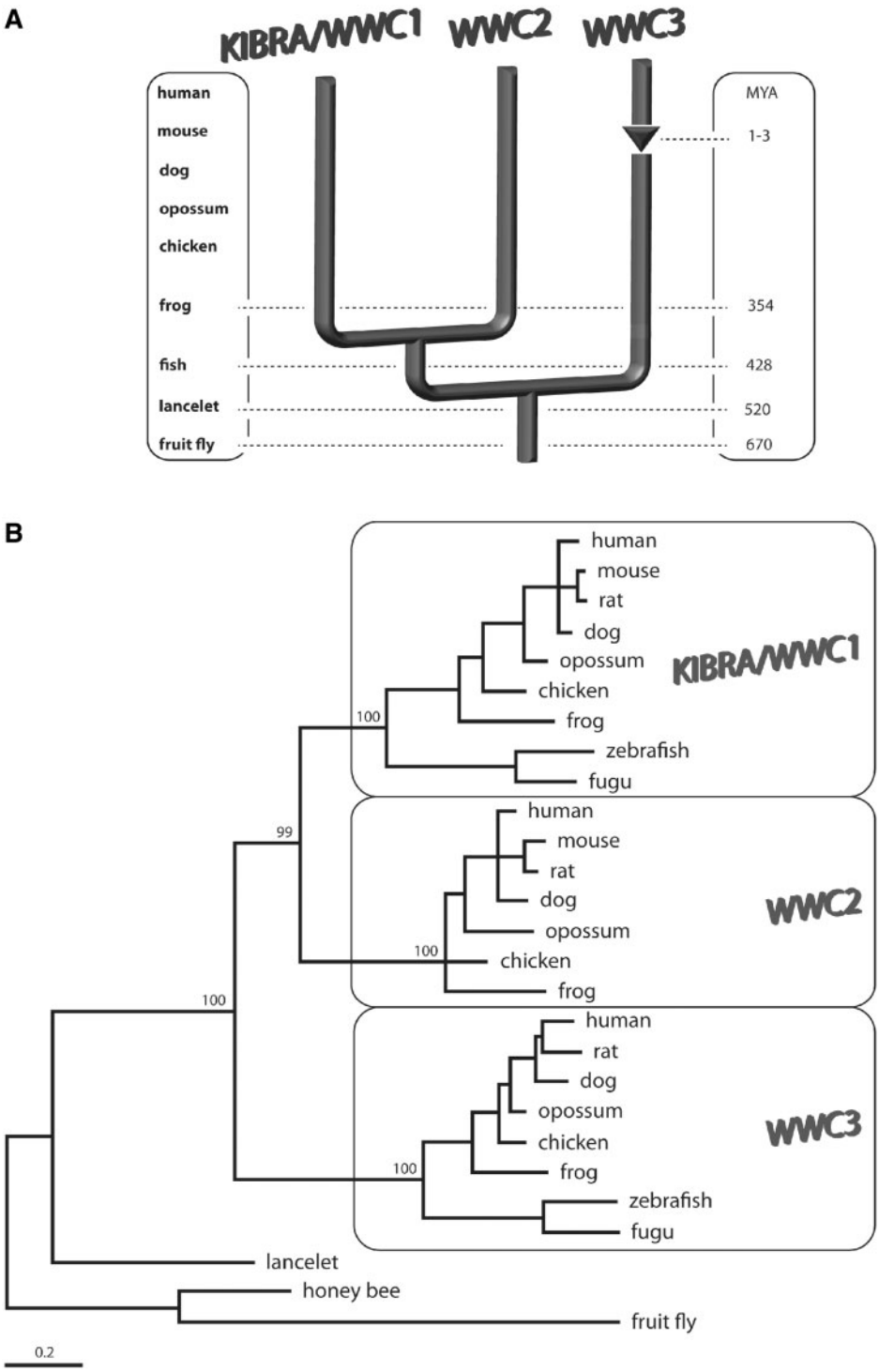

Fig. 2. Phylogenesis of the WWC protein family. (*A*) Scenario of WWC evolution. The *Drosophila* (fruit fly) and lancelet genomes contain a single WWC-like sequence (except a recently duplicated WWC sequence in the lancelet with 98.2% identity and an intact ORF in opposite orientation) that likely represents the original evolutionary situation of the WWC sequence of the ancestors of protostomes (e.g., arthropods, annelids, and mollusks) and deuterostomes (echinoderms and chordates) about 670 Ma (for dating: Ayala et al. 1998) to the common ancestor of chordates ~520 Ma (for dating: Holland et al. 2008). A second KIBRA/WWC1-like form appeared probably in the common ancestor of vertebrates about 428 Ma (for dating: Alfaro et al. 2009). Finally, all three KIBRA/WWC1-like forms (KIBRA/WWC1, WWC2, and WWC3) are present in the tetrapod ancestor ~354 Ma (for dating: Hugall et al. 2007). This pattern is consistent in all analyzed tetrapods except for the mouse (*Mus musculus*), in which the WWC3 locus and surrounding regions were deleted (black arrowhead) about 1–3 Ma (for dating: Nguyen et al. 2011). (*B*) Maximum-likelihood tree derived from the amino acid sequences of KIBRA/WWC1, WWC2, and WWC3 in different vertebrates. Two invertebrate KIBRA/WWC1-like forms (fruit fly [*D. melanogaster*], honey bee [*Apis mellifera*], and the lancelet [*Branchiostoma floridae*]) were used for outgroup comparisons. Note: the long branch of the fish KIBRA/WWC1 sequence might represent more closely the common ancestral forms of KIBRA/WWC1 and WWC2 but significantly follows the function and evolution of the KIBRA/WWC1 form. Bootstrap values for the different WWC forms and their interrelationships are indicated. Branches supported by <75% of bootstrap probability were collapsed. Branch lengths = 0.1 substitutions per site.

A comparable singular WWC-like form is present in lancelets (also known as amphioxus), indicating the WWC gene representation in the common ancestor of chordates some 520 Ma. It should be noted that a detected nearly identical copy of WWC and flanking regions indicate a recent duplication process. A second WWC-like form evolved in the common ancestor of vertebrates (a potential progenitor of KIBRA/WWC1 and WWC2). Correspondingly, fish genomes contain a WWC3-like and the potential KIBRA/WWC1/WWC2-like progenitor. Probably with the passage of these species from water to land about 400 Ma, the third form, WWC2, appeared in the common ancestor of tetrapods and is clearly detectable in amphibians and amniotes. The presence of the three WWC forms is consistent in all analyzed tetrapods with the exception of *M. musculus*, which has suffered a deletion of WWC3 and its flanking sequences about 1–3 Ma (Nguyen et al. 2001).

The evolutionary scenario derived above was also retrieved by reconstructing the sequence phylogeny of the three different WWC forms in diverse vertebrate species (fig. 2*B*). As the up to 670 Ma splits of WWC forms were impossible to reconstruct reliably from diverging DNA sequences, we compared the more conserved amino acids. The 1,681 aligned characters of 27 species revealed a stable phylogenetic tree that was confirmed using maximum parsimony, maximum likelihood, and Bayesian reconstruction methods (fig. 2*B* and supplementary fig. S4, Supplementary Material online). Applying 1,000 bootstrap replications revealed significant support for the monophyly of all WWC proteins represented in different vertebrate species. However, we suggest that the diverged KIBRA/WWC1 form of fish represents the potential KIBRA/WWC1-WWC2 progenitor. Functional constraints might have promoted a KIBRA/WWC1-like evolution of this precursor form in fish (fig. 2*A*). WWC2 could not be detected in the seven published genomes of fish species as presented at the UCSC Blat server (http://genome.ucsc.edu, last accessed April 10, 2014). On the other hand, at least traces of KIBRA/WWC1-like sequences and WWC3 were detected in all of them. Interestingly, traces of WWC2-like sequences (first exons with intact ORFs) were found at two locations in the sequenced Coelacanth genome. However, at the same time, KIBRA/WWC1- and WWC3-like sequences could not be detected in the sparsely sequenced Coelacanth genome.

We found significant evidence supporting the clustering of all representative tetrapod KIBRA/WWC1, WWC2, and WWC3 forms. As far as resolvable, the phylogenetic branching order within the three WWC clades corresponds to the phylogenetic relationships of the investigated species. A cluster merging KIBRA/WWC1 and WWC2 is significantly supported by all reconstruction methods, indicating that WWC3 diverged first among the three WWC forms.

Data from intact ORFs and derived EST indicate the presence of functional pressure on all three WWC loci. This is also well supported by a Bayesian test for selective constrains. Ninety-six percent of WWC1, 94% of WWC2, and 96% of WWC3 coding sites are under strong selection (supplementary material S11, Supplementary Material online). Because the fish KIBRA/WWC1-like form is probably close to an intermediate of KIBRA/WWC1 and WWC2, we removed this form from the relative rate test. Perhaps due to saturation effects, we found no significant values for synonymous substitutions per synonymous sites (Ks) at the DNA level. Highly significant differences of the substitution rate for nonsynonymous transversions per nonsynonymous sites (Ba; using the lancelet as an outgroup) were detected for KIBRA/WWC1 versus WWC3 (Ba1 = 0.295, Ba2 = 0.335; P_Ba = 0.00036) and WWC2 versus WWC3 (Ba1 = 0.294, Ba2 = 0.335; P_Ba = 0.00019) (supplementary material S12, Supplementary Material online). The longer branches of KIBRA/WWC1 representatives compared with those of WWC2 (fig. 2A) suggest an accelerated substitution rate of KIBRA/WWC1 (Ba1 = 0.255, Ba2 = 0.236; P_Ba = 0.019; using human WWC3 as an outgroup). However, because of saturation effects, it was not possible to prove for purifying selection using the relative rate test. A Bayesian test however indicates strong purifying selection for all three WWC genes with a slightly lower level for WWC2 ($omega^{-} = 0.050$) compared with KIBRA/WWC1 ($omega^{-} = 0.036$) and WWC3 ($omega^{-} = 0.041$) ($omega^{-}$ = dN/dS ratio for negatively selected sites) (supplementary material S11, Supplementary Material online). In this context, it is worth to note that WWC3 is one of the 114 proposed candidates that are exposed to X-inactivation and suspected to be under strong purifying selection (Zhang et al. 2013).

Tissue-Specific Expression of the WWC Family Members

KIBRA/WWC1 displays a high expression in kidney and brain of rodents and humans (Kremerskothen et al. 2003; Johannsen et al. 2008). However, there were no data available regarding the tissue-specific expression pattern of WWC2 and WWC3. We therefore performed a qRT–PCR analysis using mRNA isolated from various organs of rats. In both female and male rats, we detected a basal expression of KIBRA/WWC1, WWC2, and WWC3 in kidney, brain (cerebrum), and liver tissue at moderate levels (fig. 3 and supplementary fig. S5, Supplementary Material online) and a very high expression level in lung. In testis, mainly WWC2 was detected, whereas ovary tissue displays enhanced levels of WWC3.

WWC Proteins Form Homo- and Heterodimers and Share Common Binding Proteins

KIBRA/WWC1 is able to form head-to-tail homodimers (Johannsen et al. 2008). Due to the highly conserved protein structure among the members of the WWC family, we speculated that all WWC proteins can form both homo- and heterodimeric complexes. To verify this, we used the yeast two-hybrid system and cotransformed yeast cells with constructs encoding human KIBRA/WWC1, WWC2, or WWC3, respectively. The growth on selective media and subsequent β-galactosidase reporter assays revealed a direct pairwise interaction between KIBRA/WWC1, WWC2, and WWC3. In addition, homodimerization of WWC2 and WWC3 proteins was demonstrated (supplementary fig. S6, Supplementary Material online). Next, we aimed to confirm the presence of WWC protein heterodimeric complexes using

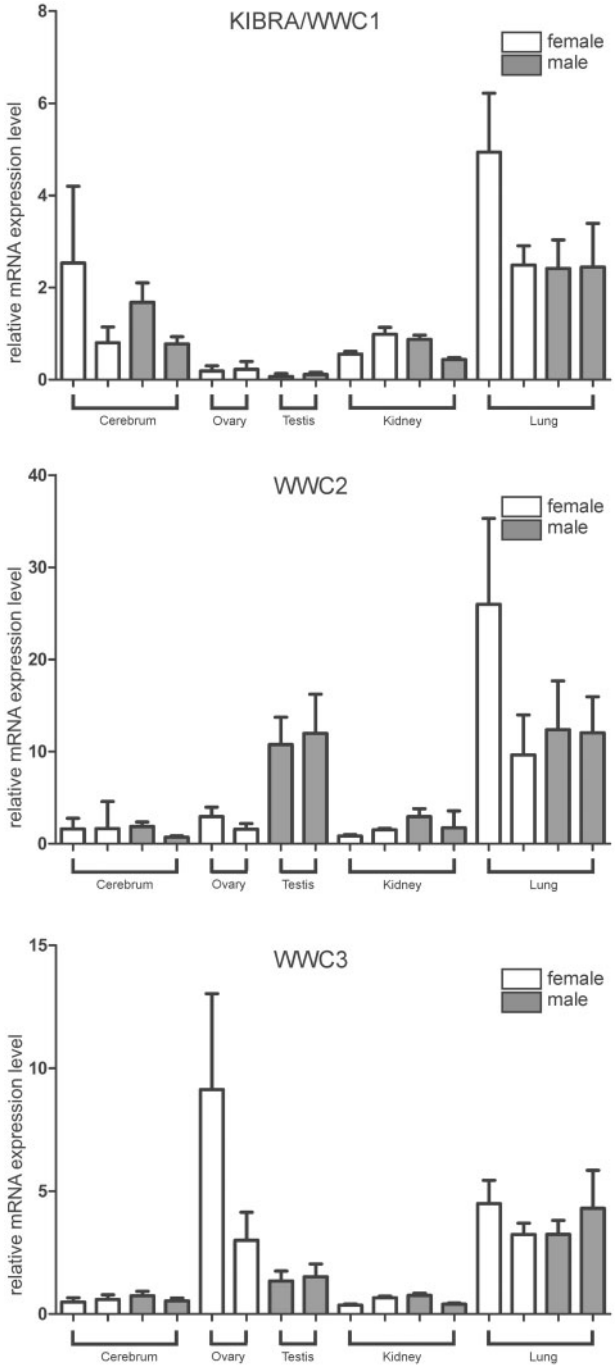

FIG. 3. Expression pattern of the three different WWC mRNAs in selected rat organs. Quantitative reverse transcription PCR (qRT–PCR) with total RNA isolated from different rat tissues shows the expression pattern of KIBRA/WWC1, WWC2, and WWC3. WWC mRNA expression was analyzed relative to the two housekeeping gene transcripts GAPDH and Cyc1. The error bars were calculated with help of the E-method LightCycler 480 II software and represent standard deviations (SDs) from triplicate samples. A complete expression pattern for WWC mRNAs in all tested organs is presented in supplementary figure S5, Supplementary Material online.

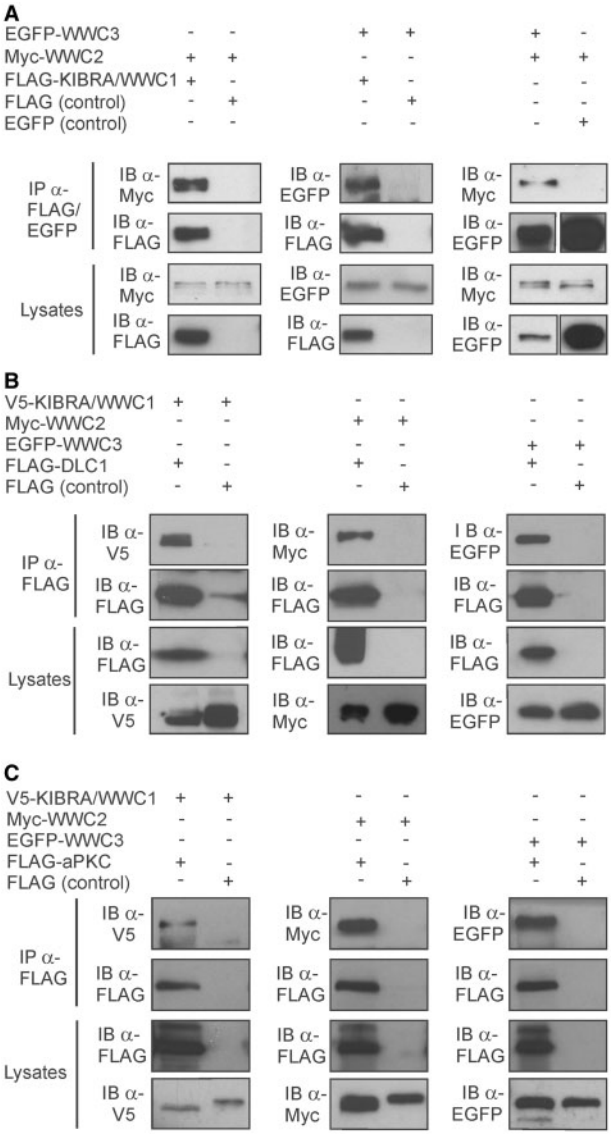

FIG. 4. Dimerization of WWC proteins and common binding partners. (*A*) WWC proteins form heterodimeric complexes. HEK293T cells were transfected with a combination of constructs encoding FLAG-KIBRA/WWC1, Myc-WWC2, or EGFP-WWC3, and CO-IP experiments were performed using cytosolic lysates. Purified complexes were analyzed by western blotting using indicated antibodies. Vectors encoding only the FLAG or the EGFP tag were used as control. (*B*) DLC1 associates with all members of the WWC protein family. HEK293T cells were cotransfected with plasmids encoding FLAG-tagged DLC1 together with V5-tagged KIBRA/WWC1, Myc-tagged WWC2, or EGFP-tagged WWC3. A plasmid encoding only the FLAG tag was used as control. CO-IP experiments with lysates from transfected cells using anti-FLAG antibodies and subsequent western blot detection revealed an interaction of DLC1 with all WWC proteins. (*C*) aPKC is a common binding partner for the WWC proteins. Cotransfection and immunoprecipitation experiments (performed as describe above) demonstrated a common binding of FLAG-tagged aPKC to KIBRA/WWC1, WWC2, and WWC3.

coimmunoprecipitation (CO-IP) studies. Therefore, we cotransfected HEK293T cells with combinations of vectors encoding Myc-, FLAG-, or green fluorescent protein (EGFP)-tagged WWC proteins and used cell lysates and immobilized anti-FLAG or anti-EGFP antibodies for CO-IP experiments and subsequent western blot analysis. Figure 4*A* shows an association between EGFP-tagged WWC3 or Myc-tagged WWC2 with FLAG-tagged KIBRA/WWC1. Furthermore, these

experiments revealed that Myc-tagged WWC2 could be coimmunoprecipitated with EGFP-tagged WWC3 but not with EGFP as a control. From these findings, we concluded that KIBRA/WWC1, WWC2, and WWC3 are able to form homo- and heterodimeric complexes.

As a scaffold protein, KIBRA/WWC1 is able to bind to diverse interaction partners, thereby affecting their function and activity in cells (Schneider et al. 2010). On the basis of their structural similarities, we speculated that the WWC proteins share a subset of binding partners. To show this, we performed CO-IP experiments with lysates from transfected HEK293T cells expressing tagged WWC proteins in combination with the known KIBRA/WWC1-binding partner DLC1 and aPKC. Our CO-IP experiments revealed a common binding of all WWC proteins to FLAG-tagged DLC1 (fig. 4*B*) and aPKC (fig. 4*C*), indicating that the association with these molecules is a common feature of the WWC protein family. In addition we could demonstrate that endogenous aPKC can be coimmunoprecipitated with all EGFP-tagged WWC proteins (supplementary fig. S7*A*, Supplementary Material online). In this context, it is worth to note that the aPKC-binding motif of KIBRA/WWC1 was recently mapped and consists of a conserved stretch of 20 amino acids containing essential arginine residues (supplementary fig. S3, Supplementary Material online; Vogt-Eisele et al. 2014). In contrast, the DLC1-binding sites within the KIBRA/WWC1 protein are not defined, yet.

Impact of WWC Proteins on Hippo Signaling

KIBRA/WWC1 negatively regulates Hippo signaling by activating LATS kinases that in turn phosphorylate YAP and prevent its nuclear import (Xiao, Chen, Ji, Dong, et al. 2011). To further characterize the role of each WWC protein in the Hippo signaling pathway, we addressed their potential binding to LATS kinases. We transfected HEK293T cells with plasmids encoding EGFP-tagged KIBRA/WWC1, WWC2, or WWC3 and analyzed the interaction of the immunoprecipitated EGFP fusion proteins with endogenous LATS1. Our results demonstrate that endogenous LATS1 binds to all EGFP-tagged proteins (fig. 5*A*). Comparable results were obtained for LATS2 (supplementary fig. S7*B*, Supplementary Material online).

On the basis of our findings that all WWC proteins interact with LATS1/2, we wanted to decipher the role of WWC proteins on LATS and YAP phosphorylation. To address this, we generated stable HEK293T cell lines that allow an inducible overexpression of KIBRA/WWC1, WWC2, or WWC3. Using western blot analysis with extracts from control and induced cells, we determined a striking temporal correlation between WWC protein expression and LATS or YAP phosphorylation (fig. 5*B*). To measure the putative impact of an enhanced WWC expression on Hippo signaling, we next performed a pGTIIC luciferase assay that was shown to sensitively respond to YAP transcriptional activity (Dupont et al. 2011). In this assay, nuclear (nonphosphorylated) YAP associates with TEAD family transcription factors, which in turn bind to concatenated TEAD-binding sites (ACATTCCA) to induce the transcription of a luciferase reporter gene. For these experiments, HEK293 cells were co-transfected with a combination of plasmids encoding YAP, LATS1 (served as a positive control) or the individual WWC member, and the pGTIIC luciferase reporter. We observed a significant reduction in luciferase activity in cells when LATS1, KIBRA/WWC1, WWC2, or WWC3 were coexpressed with YAP indicating that all three WWC proteins are negative regulators of Hippo signaling (fig. 5*C*).

Nuclear, nonphosphorylated YAP activates a conserved transcription program that induces cell proliferation and organ growth (Ikmi et al. 2014). Because of the inhibitory effect of WWC protein overexpression on Hippo signaling, we wanted to test their impact on cell proliferation. Using the well-established 3-[4,5-dimethylthiazol-2-yl]-2,5 diphenyl tetrazolium bromide (MTT) assays (see Materials and Methods), we could determine that enhanced levels of the individual WWC proteins resulted in a reduced proliferation of HEK293T cells after prolonged cultivation times (fig. 5*D*).

Human WWC Proteins Regulate Organ Growth in *Drosophila*

Overexpression of *Drosophila* KIBRA/WWC1 (DmKibra) in the compound eye has been shown to affect ommatidia formation, resulting in a "rough eye" phenotype reflecting a smaller organ size due to a reduction of ommatidia numbers (Baumgartner et al. 2010; Genevet et al. 2010; Yu et al. 2010). Our experiments revealed that this defect can be phenocopied by expression of all three human homologs (HsWWC1-3; fig. 6*A*). Furthermore, quantification of the anterior:posterior ratio of the wing area upon overexpression of DmKibra, HsKIBRA/WWC1, HsWWC2, or HsWWC3 in the posterior compartment demonstrated that increased levels of DmKibra as well as of all three human homologs resulted in a significant decrease in organ size (the anterior:posterior ratio of the wing area is decreased; fig. 6*B*). However, DmKibra exhibited the highest efficiency, whereas HsWWC3 in contrast to HsKIBRA/WWC1 and HsWWC2 showed only a moderate effect. These data underline that all three human WWC proteins are capable to modulate the Hippo pathway in vivo to regulate organ size.

Discussion

KIBRA/WWC1 represents a scaffolding protein involved in many intracellular signaling pathways including targeted vesicle transport, receptor recycling, and cytoskeleton dynamics (Schneider et al. 2010). Here, we provide novel facts for KIBRA/WWC1 and its family members WWC2 and WWC3 based on their evolutionary lineage, an expression pattern analysis in various mammalian organs, a comprehensive interaction analysis, and we obtained implications of the WWC proteins on Hippo pathway signaling.

Phylogenetic Evolution of the WWC Family

Our data from phylogenetic reconstructions reveal that the WWC family arose from one founder gene (KIBRA/WWC1-like) probably most similar to the KIBRA/

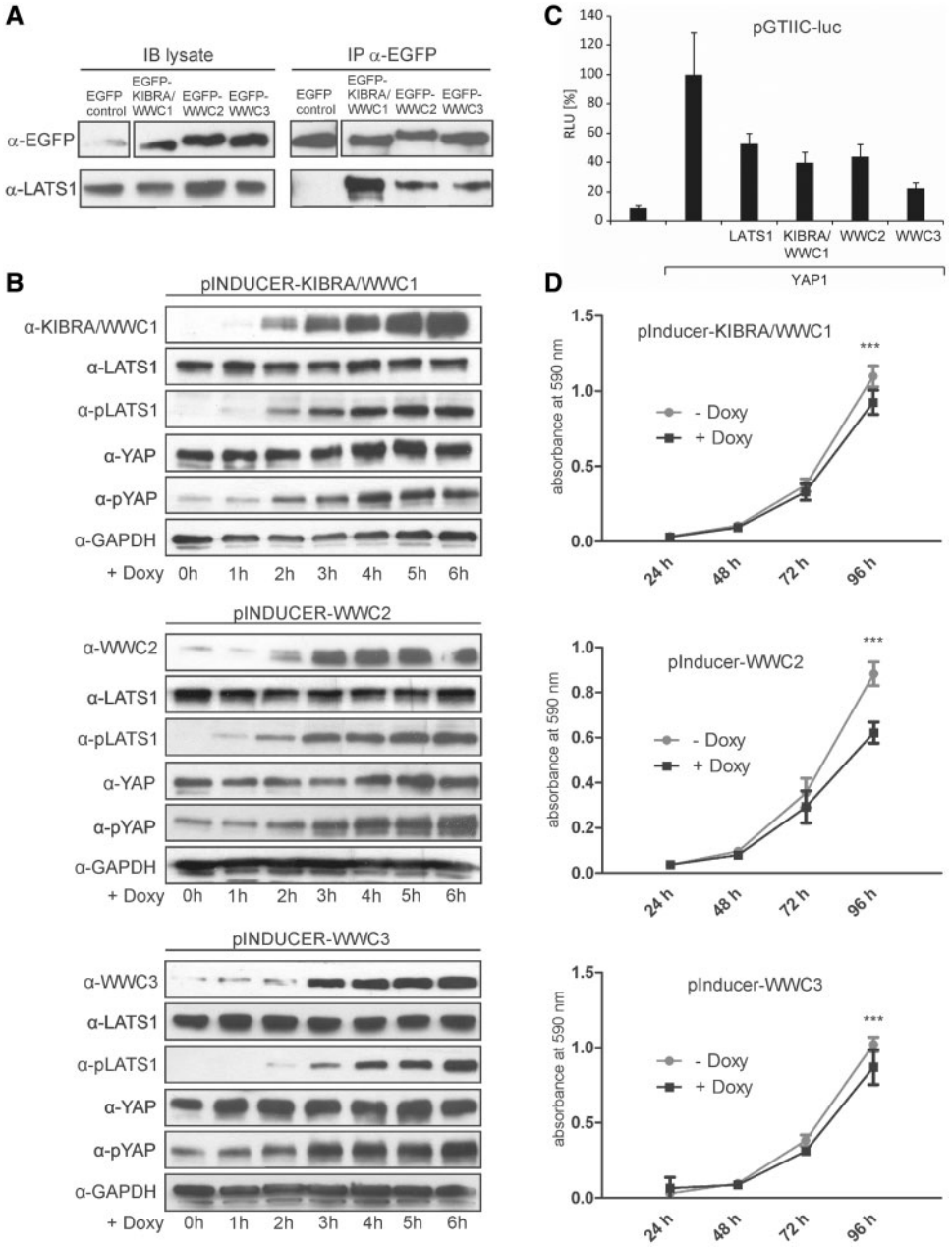

Fig. 5. Impact of WWC proteins on Hippo signaling. (*A*) Binding activities of human WWC proteins to LATS1. HEK293T cells were cotransfected with constructs encoding EGFP-tagged KIBRA/WWC1, WWC2, and WWC3, respectively. A vector expressing EGFP served as control. EGFP-trap experiments demonstrated that all WWC proteins bind to endogenous LATS1 kinase albeit with different affinities (EGFP-KIBRA/WWC1 > EGFP-WWC2 = EGFP-WWC3). (*B*) Induced overexpression of WWC proteins correlates with increased LATS and YAP phosphorylation. Overexpression of each WWC protein was induced in stable HEK293T cells using doxycycline (Doxy, 125 ng/ml) for the indicated times. Cell extracts were used for western blot analyses to detect LATS1, phospho-(p)LATS1/2, YAP, and phospho(p)-YAP. Detection of endogenous GAPDH served as a loading control. (*C*) All WWC proteins negatively regulate YAP transcriptional activity. HEK293 cells were cotransfected with indicated combinations of plasmids, together with the pGTII luciferase reporters. Luciferase activity in cell lysates was measured to demonstrate activation or inhibition of Hippo signaling. Cotransfecting LATS1 served as control for a negative regulator of Hippo signaling activity. All WWC proteins significantly reduce the transcriptional activity of YAP1. RLU denote relative luciferase units given in percent, error bars represent SD with six replicates per condition. (*D*) Overexpression of WWC proteins impairs cell proliferation. A MTT assay was used to determine cell viability and proliferation of WWC-overexpressing cells 0–96 h after doxycycline induction. Absorbance of triplicate samples was measured at 560 nm. (Mean and SD, *T*-test, $^{***}P < 0.0001$ for KIBRA/WWC1 and WWC2, $P = 0.0004$ for WWC3, 8–12 replicates per condition).

WWC1-like form in invertebrates (*Drosophila*, fig. 2*A* and *B*). During evolution, two WWC genes, KIBRA/WWC1-like and WWC3, arose in the ancestor of vertebrates (today still represented by the fish genome). However, we cannot fully exclude the scenario of a WWC2 deletion in the ancestral fish. However, no traces of WWC2 could be detected in any of the seven published fish genomes. Interestingly, traces of two copies of WWC2-like sequences are present in the coelacanth,

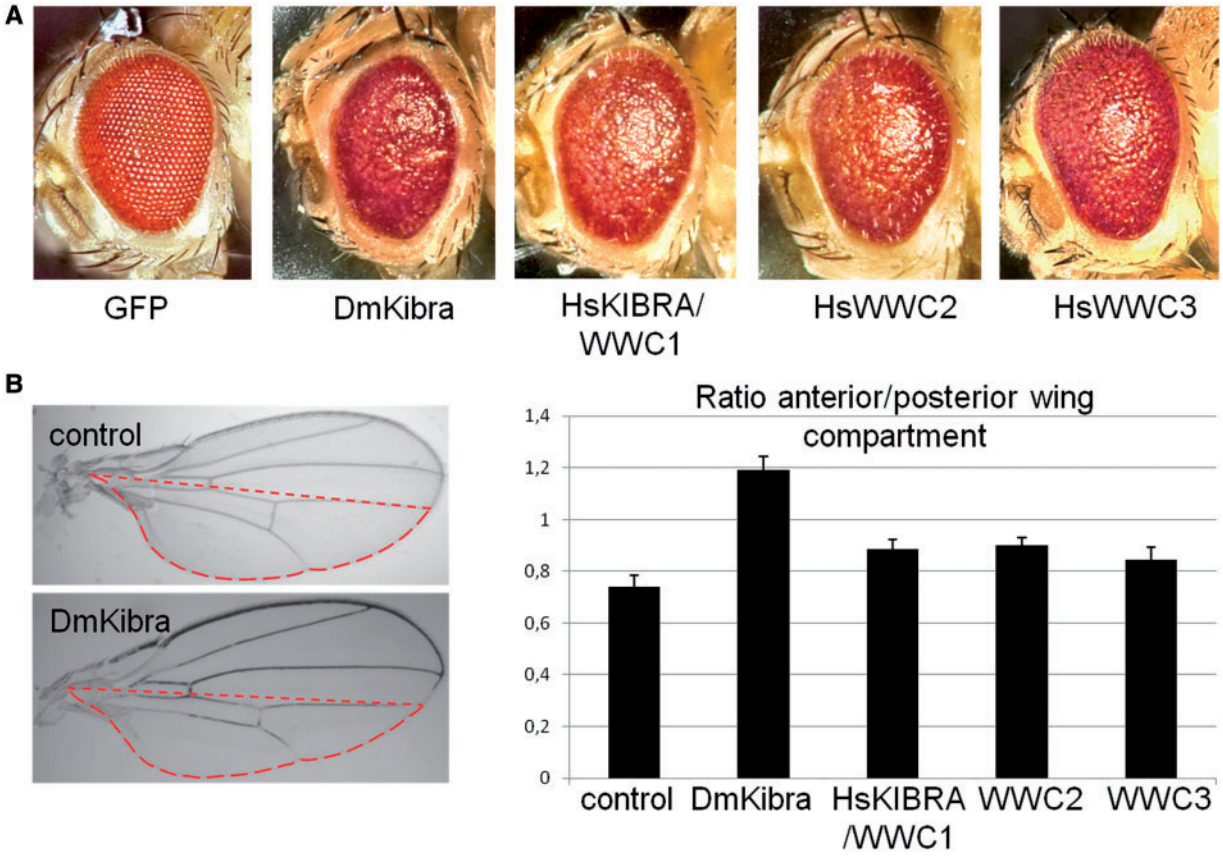

FIG. 6. Human WWC proteins affect eye development and organ size in *Drosophila*. (*A*) Overexpression of the human WWC proteins (HsWWC1-3) in the *Drosophila* eye results in morphology defects similar to overexpression of *Drosophila* Kibra (DmKibra). GFP served as negative control. (*B*) Human WWC proteins regulate organ size in the *Drosophila* wing. DmKibra or HsWWC1-3 was expressed in the posterior compartment (framed area) of the wing using en::GAL4. The ratio between anterior and posterior wing area was calculated and indicated. (DmKIBRA $P < 0.0001$, HsWWC1/KIBRA $P < 0.0001$, HsWWC2 $P < 0.0001$, HsWWC3 $P = 0.001$).

a group outside of ray-finned fishes closely related to lungfish and tetrapods. Possibly WWC2 evolved in the common ancestor of these three groups (represented by the fish genome). Finally, in tetrapods, the KIBRA/WWC1-like gene was split to form the later KIBRA/WWC1 and WWC2 genes that are expressed together with WWC3. Due to a chromosomal deletion, *M. musculus* has lost the Wwc3 gene locus. However, the deletion is specific only to *M. musculus*, and WWC3 is still present in other rodents, such as the close relative *Mus spretus* and rat. *M. musculus* and *M. spretus* separated about 1–3 Ma, and the genomic deletion therefore can be regarded as a relatively recent event (Nguyen et al. 2011). The absence of the WWC3 gene in *M. musculus* suggests that WWC3 is not essential for survival, at least in this lineage. Nevertheless, selection pressure is strongly exerted on WWC3, but these signals may also be remnants of a potentially stronger functional pressure in ancient times, for example, before emergence of the related forms followed by functional relaxation for WWC3. In general, the significantly smaller size of the mouse genome (14% less than the human genome) indicates a high rate of deletions in the mouse lineage (Mouse Genome Sequencing Consortium; Waterston et al. 2002). Moreover, Jaillon et al. (2004) proposed a whole-genome duplication in the teleost fish lineage. However, we could not find any additional WWC copies in the published *T. nigroviridis* genome, suggesting possible gene loss in the fish lineage.

Expression Pattern and Molecular Features of the WWC Proteins

In rats, all WWC genes share a common expression in the brain, the kidney, the liver, and the lung (fig. 3). This observation provides first evidence that the different WWC proteins may fulfill similar roles in these organs. Remarkably, we detected that WWC2 is highly expressed in rat testis whereas ovary tissues display mainly WWC3 mRNA. At present, we can only speculate that this enhanced expression of the individual WWC member in reproductive organs is linked to a tissue-specific function.

Our in vitro protein interaction studies revealed that the WWC proteins are able to form hetero- or oligomeric complexes, and they all can associate with the known KIBRA/WWC1 binding partners DLC1 and aPKC (fig. 4 and supplementary figs. S6 and S7*A*, Supplementary Material online). This may suggest the presence of a putative WWC protein network that might be involved in the regulation of intracellular processes. Moreover, it is likely that the individual WWC family members share a common molecular function, for

example, for protein recruitment, vesicle transport, or cell polarity.

Impact of the WWC Proteins on Hippo Signaling

The Hippo pathway represents one of only few signaling systems that are crucial for the development of all metazoan. Remarkably, not only the protein sequences but also the complex interplay between the key components (e.g., LATS/Warts, YAP/Yorkie, and NF2/Merlin) within the Hippo pathway display a high degree of evolutionary conservation (Hilman and Gat 2011; Zhu et al. 2013; Ikmi et al. 2014).

Our findings further elucidate the conserved role of the WWC family as negative regulators in Hippo signaling. We could demonstrate that all WWC proteins enhance phosphorylation of LATS and YAP (fig. 5*B*), reduce the transcriptional activity of YAP (fig. 5*C*), and impair cell proliferation (fig. 5*D*). Interestingly, at least KIBRA/WWC1 and WWC2 may also act as components of a conserved inhibitory feedback loop within the Hippo pathway as their genes were shown to represent targets of YAP transcriptional activity (Xiao, Chen, Ji, Dong, et al. 2011; Judson et al. 2012).

Do the different WWC proteins have a common impact on organ growth control as shown before for DmKibra? To analyze this, we used an overexpression approach of human WWC proteins in the eyes and wings of flies. Overexpression of all three human WWC proteins showed similar (although weaker) effects as DmKibra: a rough eye phenotype as well as a reduction of the posterior wing size compartment (fig. 6; Baumgartner et al. 2010; Genevet et al. 2010; Yu et al. 2010). These observations indicate that the ability of the WWC proteins to modulate the Hippo pathway, to inhibit cell proliferation, and to regulate tissue growth is evolutionarily conserved from fly to men. Furthermore, our data demonstrate that increased levels of WWC proteins can both activate the Hippo pathway in cell culture models and regulate organ growth in vivo underpinning the pathway's strong conservation. In terms of cell proliferation control and tumor suppression, a comparable evolutionary conservation was already described for the Discs large/Lethal (2) giant larvae/Scribble complex (Grifoni et al. 2004; Elsum et al. 2012) or Liver kinase B 1 (LKB1) complex (Shorning and Clarke 2011).

Our data clearly support the role of the WWC family as negative regulators of cell proliferation and organ growth. However, recent reports must be mentioned, demonstrating that the proliferation and malignancy of cancer cells positively correlate with high levels of KIBRA/WWC1. For example, in human gastric cancer, a high expression of KIBRA/WWC1 together with low levels of aPKC was associated with increased cell proliferation, enhanced tumor invasion, and poor prognosis (Yoshihama et al. 2013). Interestingly, in breast cancer cells not only the enhanced expression level but also the RSK-mediated phosphorylation of KIBRA/WWC1 is crucial for its positive effect on proliferation (Yang et al. 2014).

WWC3—The Peculiar One of the WWC Family

Our data indicate a specific role of WWC3 within the WWC family. During evolution, WWC3 was separated early from KIBRA/WWC1 and WWC2. Selection pressure was strongly exerted on the WWC3 gene possibly due to an important function in ancient times. As WWC3 is not expressed in *M. musculus*, this protein seems to be dispensable for survival but may be involved in the fine-tuning of cellular processes in higher mammals. This is underlined by recent findings demonstrating that a single-nucleotide polymorphism within the human WWC3 gene is linked to mental retardation that may point to a specific function of WWC3 in higher brain function (Jiang et al. 2013).

In contrast to the KIBRA/WWC1 and WWC2 genes that are located on autosomes, the WWC3 gene is mapped to the short arm of the X chromosome in mammalian genomes (Nguyen et al. 2011). This is important in terms of chromosomal regulation as X-linked gene activity is controlled by specific epigenetic mechanisms including an X upregulation in both sexes to balance expression of autosomal and X-linked genes as well as an X inactivation of one allele in females (Nguyen et al. 2011).

The WWC Family as a Novel Example for Genetic Redundancy?

Our data about the common function of the individual WWC protein in Hippo signaling clearly point to genetic redundancy within the WWC gene family. This evolutionary phenomenon is occasionally observed in genetic knockout strategies in model organisms where the inactivation of a gene does not lead to a phenotypic effect likely due to compensation by another member of the same gene family (Zhang 2012). A prominent example for this effect is the Src gene family that encodes related tyrosine kinases crucial for the control of cell proliferation (Stein et al. 1994). Earlier observations and the data presented here provide evidence that the WWC gene family is a novel candidate for genetic redundancy and a natural knockout (WWC3 in *M. musculus*), too. This is especially illustrated by the fact that the evolutionary loss of the WWC3 gene in the *Mus* lineage showed no detectable phenotypic effects. Furthermore, a genetic ablation of KIBRA/WWC1 in *M. musculus* resulted only in a mild cognitive phenotype without remarkable deficits in kidney or lung function (Makuch et al. 2011; Vogt-Eisele et al. 2014). So, although these genetically modified mice express only WWC2 as the remaining member of the WWC family, this has no crucial consequences for survival.

Our experiments in *Drosophila*, wherein the overexpression of each of the human WWC protein led to a comparable phenotype (rough eyes, decreased wing growth) further supports a redundant function within the WWC family. However, if the WWC genes represent another example for genetic redundancy, it remains to be determined why and how they escaped from natural selection during evolution.

Taken together, we provide the first evolutionary, molecular, and functional analysis of the WWC gene family, setting

the basis for further studies that will embark on the underlying molecular mechanisms of WWC gene function.

Materials and Methods

Reagents

Culture media and cell culture antibiotics were obtained from PAA (Coelbe, Germany) and Invitrogen (Mannheim, Germany). Standard highest grade reagents were from Sigma–Aldrich (Deisenhofen, Germany).

Cloning of the ORF for Human WWC3

GenBank Acc. No. NM_015691 represents a human WWC3 cDNA encoding a protein of 1092 amino acids (aa) lacking the representative amino-terminal WW domains found in KIBRA/WWC1 and WWC2. The NM_015691 sequence seems to be truncated at the 5′-end because the cDNA of the two nonhuman primates *Papio anubis* (NCBI GenBank Acc. No. XM_003917391) and *Callithrix jacchus* (XM_002762604) encode longer WWC3 proteins (1,218 aa and 1,207 aa, respectively) containing two WW domain at the amino terminus. In addition, two human EST sequences, BU500742 and BU500300, overlap with NM_015691 at the 5′-end and encode for protein fragments highly similar to the amino terminus of *P. anubis* WWC3. We therefore cloned the full-length ORF from human WWC3 by PCR using a placenta cDNA library (Invitrogen) as template, the Accuprime DNA polymerase for GC-rich sequences (Invitrogen), a forward primer (5′-atgccttggctgagcggcgg-3′) corresponding to the BU500742 EST sequence and a reverse primer (5′-tcagacgtcgtcggctgggag-3′) corresponding to the NM_015691 sequence. Sequencing of the PCR product revealed a cDNA of 3,654 nucleotides (including the stop codon) encoding a WWC3 protein of 1,217 amino acids (GenBank Acc. No. KC987947; supplementary fig. S1, Supplementary Material online).

Constructs and Antibodies

cDNAs encoding human KIBRA/WWC1, WWC2, and WWC3 were amplified by PCR from human placenta cDNA library (Invitrogen) using specific primers with adjacent restriction sites and were cloned into Gateway Entry (pENTR-D/TOPO, Invitrogen) and Destination vectors (pDEST22, pDEST32, Invitrogen), V180 pLP Triple-FLAG (addgene, plasmid 11707, for expression of 3xFLAG-WWC3), pINDUCER-puro based on pINDUCER-21 (Meerbrey et al. 2011), pEGFP-C1-3, pAS-2-1, and pACTII yeast two hybrid vectors (Invitrogen). Mouse monoclonal antibodies directed against EGFP (JL8), the FLAG tag (M2), or the Myc tag (9E10) were purchased from Invitrogen or Sigma–Aldrich, respectively. Monoclonal mouse antibody directed against YAP was from SantaCruz (Heidelberg, Germany). Antibodies against LATS1 (3477), LATS2 (5888), p-LATS1-T1079 (8654), and p-YAP-S127 (4911) were purchased from Cell Signaling (Frankfurt, Germany). Antibodies against GAPDH were from Covance, USA (MMS-580). Fluorochrome-conjugated secondary antibodies coupled to the fluorescent dyes Alexa 488 and 594 were purchased from Invitrogen. Horseradish peroxidase-conjugated secondary antibodies were purchased from Dianova (Hamburg, Germany).

Polyclonal antibodies directed against *Escherichia coli* BL21-produced, recombinant human KIBRA/WWC1 (aa 661–796), WWC2 (aa 698–825), and WWC3 (aa 725–852) were generated by immunization of rabbits (EUROGENTEC, Cologne, Germany) and were purified by affinity chromatography.

Cell Transfection, Extract Preparation, and Western Blotting

Human HEK293T cells were cultivated and transfected using calcium phosphate precipitation as described previously (Kremerskothen et al. 2003; Duning et al. 2008). Cellular lysates were prepared by scraping cells 16-h posttransfection into IP buffer (1% Triton-X 100, 20 mM Tris–HCl [pH 7.5], 25 mM NaCl, 50 mM NaF, 15 mM $Na_4P_2O_7$, and 1.5 mM EDTA) containing protease inhibitors (*Complete*; Roche, Mannheim, Germany). Lysates were centrifuged at 10,000 × g for 45 min at 4 °C to pellet cell debris and nuclei. Supernatants were removed and stored at −80 °C until further use. Extracts from inducible cells were generated by scraping the cells directly into Laemmli sample buffer. Sodium dodecyl sulfate–polyacrylamide gel electrophoresis (SDS–PAGE) and western blotting analysis were performed using standard techniques (Duning et al. 2008).

Lentiviral Transduction and Generation of Inducible Cell Lines

Stable, doxycycline-inducible cell lines were obtained using a modification of the recently established lentiviral pINDUCER system (Meerbrey et al. 2011; Schulze et al. 2014). In brief, HEK293T cells were cotransfected using calcium phosphate precipitation with the individual pINDUCER21puro-KIBRA/WWC1, WWC2, or WWC3 constructs (pINDUCER21-puro contains a puromycin resistance cassette instead of the EGFP-coding region of the pINDUCER21 plasmid) together with psPAX2 (addgene, plasmid 12260) and pMD2.G (addgene, plasmid 12259). The culture medium was changed after 6–8 h and transfected HEK293T cells were grown for additional 72 h. Afterward, the lentivirus-containing cell culture supernatant was collected and filtered through a sterile 0.45-μm syringe-driven filter unit (Millipore). Subsequently, HEK293T cells were infected for 24 h with the filtrate supplemented with polybrene (final concentration 8 μg/ml). Next, the virus-containing supernatant was replaced by fresh medium and cells were grown for 24 h. This infection procedure was repeated once.

Virus-transduced cells were selected by puromycin treatment (4 μg/ml, Sigma–Aldrich) for 7 days. Overexpression of the individual WWC proteins in the selected cell populations was induced by the addition of doxycycline (125 ng/ml) to the culture medium and was verified by western blot analysis.

MTT Assay

To measure cell proliferation and viability, a MTT assay was used as described earlier (Mosmann 1983). In brief, inducible

HEK293T cells (25,000 cells/well; 100 µl medium/well) were cultured in 96-well plates and were treated with doxycycline (125 ng/ml) for various time periods (0–96 h) to express recombinant KIBRA/WWC1, WWC2, or WWC3. Then, 10 µl MTT (Sigma–Aldrich) solution (5 mg/ml) was added to each well and the plates were incubated at 37 °C for 3 h. The formed formazan crystals were resolved in solubilization buffer (dimethylformamide, DMF) by incubation on a rocking platform for 15 min. The absorbances of the samples (8–12 samples per time point) at 590 nm were determined using a Tecan photometer (Crailsheim, Germany).

Coimmunoprecipitation

For CO-IP assays, aliquots of lysates from transfected HEK293T cells were incubated with anti-FLAG affinity beads (M2, Sigma–Aldrich) or GFP-Trap beads (Chromotek, Planegg-Martinsried, Germany) overnight at 4 °C or 1–2 h at room temperature on a rocking platform. Afterward, the beads were washed five times in IP buffer. For elution of bound proteins, beads were resolved in Laemmli sample buffer and boiled for 5 min at 95 °C. Eluted immunoprecipitates were subjected to SDS–PAGE and western blot analysis.

pGTII Luciferase Assays

YAP transcriptional activity was measured using a luciferase assay based on the pGL3b_8xGTIIC-luciferase plasmid obtained from addgene (plasmid #34615) (Dupont et al. 2011). Expression plasmids for FLAG-tagged YAP1, LATS1, KIBRA, and WWC2 were constructed by recombining an Entry vector (either based on pDONR-Zeo or pDONR207) carrying the corresponding ORF into a Gateway Destination vector for N-terminal fusions pcDNA3.1_FLAG_DEST (based on pCDNA3.1 from Invitrogen) for YAP1 and pCMV7.1_3xFLAG_DEST (based on pCMV7.1_3xFLAG from Sigma) for LATS1, KIBRA, and WWC2. The V180 pLP Triple FLAG plasmid to express 3xFLAG-WWC3 was described above. Luciferase assays were performed in a 96-well format using HEK293 cells and Lipofectamine2000 as transfection reagent. A *Renilla* luciferase mix consisting of plasmids coding for CMV-hRL, TK-hRL, and SV40-hRL at a molar proportion of 1:2:10 (Wehr et al. 2006) served as control. Each well was transfected with equal amounts of DNA (20 ng each for pGL4_6xUAS-luc2 (based on pGL4.20_luc2/Puro from Promega; UAS: upstream activating sequence), pGL3b_8xGTIIC-luciferase, stimulus plasmids (i.e., containing FLAG-YAP1, 3xFLAG-KIBRA/WWC1, 3xFLAG-WWC2, and 3xFLAG-WWC3), and 20 ng *Renilla* mix. Empty pcDNA3.1 was used to equalize DNA amounts. Firefly (luc) and *Renilla* luciferase activities were measured in a Mithras LB940 luciferase reader (Berthold Technologies; Bad Wildbad, Germany) using the Dual-Luciferase Reporter Assay System (Promega, Heidelberg, Germany). RLU denote relative luciferase units given in percent, error bars represent SD with six replicates per condition.

Yeast Two-Hybrid System

For intracellular protein binding experiments, the yeast two-hybrid system was used as described earlier (Kremerskothen et al. 2003). In brief, Y190 yeast cells were cotransformed with corresponding bait/prey constructs. Direct interactions of recombinant fusion proteins were detected by growth of transformed cells on selective media and by β-galactosidase filter (LacZ) assays.

Drosophila Experiments

The coding regions for *D. melanogaster* Kibra (DmKibra; gift from Nic Tapon) and human (Hs) WWC1-3 were subcloned into a modified gateway vector containing a ubiquitous promoter (Ubiquitin), a 6xMyc-Tag and an attB-site (Sen et al. 2012). Phi-C31-mediated integrase was used to establish transgenic flies using attP40 (Groth et al. 2004). Overexpression constructs were generated using a pUASt-GFPattB vector, and transformants were established using attP40. The UAS/GAL4-system (Brand and Perrimon 1993) with GMR::GAL4 and en::GAL4 (both obtained from Bloomington stock collection, Indiana University, USA) was used to overexpress DmKibra or WWC proteins in the eye and posterior wing compartment. Representative pictures of transgenic *Drosophila* eyes and wings were taken with an Axio Imager (Zeiss, Oberkochem, Germany). For wing compartment ratio, wings from at least ten males were measured and calculated as described earlier (Genevet et al. 2009).

RNA Isolation from Rat Tissues and Reverse Transcription

Three-month-old Sprague-Dawley rats (two males and two females) were sacrificed via CO_2 inhalation. Corresponding organs were removed and directly subjected to RNA purification using the Trizol method. Tissue samples from different organs were homogenized with the help of Micropestle (Eppendorf, Germany) in 1 ml Trizol Reagent (Invitrogen/Thermo Scientific, Germany) per 100 mg of tissue, and RNA isolation was carried out according to manufacturer's recommendation. Nanodrop ND-1000 spectrophotometer (Thermo Scientific, Germany) was used to quantify RNA concentrations. RNA samples were evaluated for their integrity and amount using the Bioanalyzer 2100 (Agilent Technologies). RNA samples were treated with DNase I as recommended by manufacturer prior to reverse transcription. Reverse transcription was performed using the Transcriptor high-fidelity cDNA synthesis kit (Roche Diagnostics, Germany) according to manufacturer's recommendation. RNA (5 µg) was reverse transcribed in a 20-µl reaction using random hexamer primers and protector RNase inhibitor (Thermo Scientific, Germany).

qPCR Reaction and Analysis

The qPCR reactions were carried out in 20-µl volumes using 2× LightCycler Master Mix (Roche), 0.5 µl cDNA, 4 pM each primer, and 2 pM probe. All qPCR experiments were performed according to the MIQE criteria (Bustin et al. 2009). mRNA levels were analyzed using the TaqMan qRT–PCR

assays (see supplementary tables S8 and S9, Supplementary Material online) on the LightCycler 480 II (Roche Diagnostics, Germany). Intron spanning TaqMan qPCR assays were designed using the Universal Probe Library and WEB-based site of Roche Diagnostics. Each cDNA sample was measured in triplicate and analyzed relative to two housekeeping gene transcripts (GAPDH, Cyc1) using the E-method LightCycler 480 II software (Roche Diagnostics, Germany). Results from different experiments were normalized to expression of the positive control (calibrator probe).

Reconstruction of the WWC Gene Evolution

The annotated KIBRA-like sequences WWC1–3 were downloaded from NCBI (for accession numbers, see supplementary material S10, Supplementary Material online). The amino acid sequences were aligned using MUSCLE (http://www.ebi.ac.uk/Tools/msa/muscle/, last accessed April 10, 2014) for 27 species and 1,681 characters (Edgar 2004). The DNA alignment for 27 species and 5,046 characters (including the stop codon) was performed with the RevTransServer (http://www.cbs.dtu.dk/services/RevTrans/, last accessed April 10, 2014), using the previously generated amino acid alignment as a profile and keeping an intact codon structure. Both alignments are available as supplementary material S10, Supplementary Material online.

Phylogenetic Reconstructions

MEGA5 was applied to determine the optimal substitution model for the underlying amino acid sequence data (Tamura et al. 2011). Within MEGA5, we used the JTT model with five rate heterogeneity categories (Jones et al. 1992) to reconstruct the maximum-likelihood tree (fig. 2*B*). MrBayes 3.2 was applied to derive a Bayesian tree under the JTT substitution model with five rate heterogenity categories. The tree and parameters are given in supplementary figure S4*A*, Supplementary Material online. A maximum parsimony tree was generated using PAUP 4.0b10 (Wilgenbusch and Swofford 2003) applying standard settings (supplementary fig. S4, Supplementary Material online). All three applied reconstruction methods (maximum likelihood, Bayesian reconstruction, and maximum parsimony) were used by including 1,000 bootstrap steps or corresponding Bayesian clade credibility calculations resulted in the almost same tree topology illustrated in figure 2*B*.

Relative Rate Test

RRTree (Robinson-Rechavi and Huchon 2000) was used to determine substitution shifts among KIBRA/WWC1, WWC2, and WWC3. The relative rate test was applied for DNA sequences (see above) of the seven representative species for KIBRA/WWC1 (excluding fishes because of their unclear association to KIBRA/WWC1—see above) and WWC2 and the eight species for WWC3 using the lancelet as the closest outgroup. A similar comparison was applied for human only and KIBRA/WWC1 versus WWC2 using human WWC3 for outgroup comparison. Corresponding to the consensus topology of figure 2*A*, a Newick user tree was built in MEGA5 (for Newick notation, see http://evolution.genetics.washington.edu/phylip/newicktree.html, last accessed April 10, 2014). This tree topology was to derive branch-specific substitution rates (supplementary material S12, Supplementary Material online).

Detection of Constraining Selection

MrBayes 3.2 was used to identify the selection pressure on coding sequences. To exclude highly variable positions from the DNA alignment, Gblocks was used by applying default block parameters and allowing gap positions "With Half" reducing the data set to 2,694 characters (Talavera and Castresana 2007). Just species with all three genes of WWC were included (human, rat, dog, opossum, chicken, and frog).

Supplementary Material

Supplementary figures, tables, and materials S1–S12 are available *at Molecular Biology and Evolution* online (http://www.mbe.oxfordjournals.org/).

Acknowledgments

We thank Nina Meyer, Birgit Burde, and Birte Seeger for their excellent technical assistance and all members of the Department for Molecular Nephrology for discussing the results. We are grateful to Jeffry D. Hohlman (Bristol, UK), Tony Pawson (Toronto, Canada), and Thomas Westbrook (Houston, TX) for providing plasmids. This work was supported by a grant from the Medical Faculty of the University of Muenster (IZKF, SEED 02/12 Wennmann) and DFG, SCHM1469/3-2 for J.S.

References

Alfaro ME, Santini F, Brock C, Alamillo H, Dornburg A, Rabosky DL, Carnevale G, Harmon LJ. 2009. Nine exceptional radiations plus high turnover explain species diversity in jawed vertebrates. *Proc Natl Acad Sci U S A.* 106:13410–13414.

Ayala FJ, Rzhetsky A, Ayala FJ. 1998. Origin of the metazoan phyla: molecular clocks confirm paleontological estimates. *Proc Natl Acad Sci U S A.* 95:606–611.

Baumgartner R, Poernbacher I, Buser N, Hafen EH. 2010. The WW domain protein Kibra acts upstream of Hippo in *Drosophila*. *Dev Cell.* 18:309–316.

Brand AH, Perrimon N. 1993. Targeted gene expression as a means of altering cell fates and generating dominant phenotypes. *Development* 118:401–415.

Bustin SA, Benes V, Garson JA, Hellemans J, Huggett J, Kubista M, Mueller R, Nolan T, Pfaffl MW, Shipley GL, et al. 2009. The MIQE guidelines: minimum information for publication of quantitative real-time PCR experiments. *Clin Chem.* 55:611–622.

Dong J, Feldmann G, Huang J, Wu S, Zhang N, Comerford SA, Gayyed MF, Anders RA, Maitra A, Pan D. 2007. Elucidation of a universal size-control mechanism in *Drosophila* and mammals. *Cell* 130: 1120–1133.

Duning K, Schurek EM, Schluter M, Bayer M, Reinhardt HC, Schwab A, Schaefer L, Benzing T, Schermer B, Saleem MA, et al. 2008. KIBRA modulates directional migration of podocytes. *J Am Soc Nephrol.* 19: 1891–1903.

Duning K, Wennmann DO, Bokemeyer A, Reissner C, Wersching H, Thomas C, Buschert J, Guske K, Franzke V, Flöel A, et al. 2013. Common exonic missense variants in the C2 domain of the human KIBRA protein modify lipid binding and cognitive performance. *Transl Psychiatry.* 3:e272.

Dupont S, Morsut L, Aragona M, Enzo E, Giulitti S, Cordenonsi M, Zanconato F, Le Digabel J, Forcato M, Bicciato S, et al. 2011. Role of YAP/TAZ in mechanotransduction. *Nature* 474:179–183.

Edgar RC. 2004. MUSCLE: a multiple sequence alignment method with reduced time and space complexity. *BMC Bioinform.* 5:113.

Elsum I, Yates L, Humbert PO, Richardson HE. 2012. The Scribble–Dlg–Lgl polarity module in development and cancer: from flies to man. *Essays Biochem.* 53:141–168.

Genevet A, Polesello C, Blight K, Robertson F, Collinson LM, Pichaud F, Tapon N. 2009. The Hippo pathway regulates apical-domain size independently of its growth-control function. *J Cell Sci.* 122: 2360–2370.

Genevet A, Wehr MC, Brain R, Thompson BJ, Tapon N. 2010. Kibra is a regulator of the Salvador/Warts/Hippo signaling network. *Dev Cell.* 18:300–308.

Grifoni D, Garoia F, Schimanski CC, Schmitz G, Laurenti E, Galle PR, Pession A, Cavicchi S, Strand D. 2004. The human protein Hugl-1 substitutes for *Drosophila* lethal giant larvae tumour suppressor function in vivo. *Oncogene* 23:8688–8694.

Groth AC, Fish M, Nusse R, Calos MP. 2004. Construction of transgenic *Drosophila* by using the site-specific integrase from phage phiC31. *Genetics* 166:1775–1782.

Harvey KF, Zhang X, Thomas DM. 2013. The Hippo pathway and human cancer. *Nat Rev Cancer.* 13:246–257.

Hilman D, Gat U. 2011. The evolutionary history of YAP and the hippo/YAP pathway. *Mol Biol Evol.* 28:2403–2417.

Holland LZ, Albalat R, Azumi K, Benito-Gutiérrez E, Blow MJ, Bronner-Fraser M, Brunet F, Butts T, Candiani S, Dishaw LJ, et al. 2008. The amphioxus genome illuminates vertebrate origins and cephalochordate biology. *Genome Res.* 18:1100–1011.

Hugall AF, Foster R, Lee MS. 2007. Calibration choice, rate smoothing, and the pattern of tetrapod diversification according to the long nuclear gene RAG-1. *Syst Biol.* 56:543–563.

Ikmi A, Gaertner B, Seidel C, Srivastava M, Zeitlinger J, Gibson MC. 2014. Molecular evolution of the Yap/Yorkie proto-oncogene and elucidation of its core transcriptional program. *Mol Biol Evol.* 31(6):1375–1390.

Jaillon O, Aury J-M, Brunet F, Petit JL, Stange-Thomann N, Mauceli E, Bouneau L, Fischer C, Ozouf-Costaz C, Bernot A, et al. 2004. Genome duplication in the teleost fish *Tetraodon nigroviridis* reveals the early vertebrate proto-karyotype. *Nature* 43:946–957.

Jiang YH, Yuen RK, Jin X, Wang M, Chen N, Wu X, Ju J, Mei J, Shi Y, He M, et al. 2013. Detection of clinically relevant genetic variants in autism spectrum disorder by whole-genome sequencing. *Am J Hum Genet.* 93:249–263.

Johannsen S, Duning K, Pavenstadt H, Kremerskothen J, Boeckers TM. 2008. Temporal-spatial expression and novel biochemical properties of the memory-related protein KIBRA. *Neuroscience* 155: 1165–1173.

Jones DT, Taylor WR, Thornton JM. 1992. The rapid generation of mutation data matrices from protein sequences. *Comput Appl Biosci.* 8: 275–282.

Judson RN, Tremblay AM, Knopp P, White RB, Urcia R, De BC, Zammit PS, Camargo FD, Wackerhage H. 2012. The Hippo pathway member Yap plays a key role in influencing fate decisions in muscle satellite cells. *J Cell Sci.* 125:6009–6019.

Jukam D, Desplan C. 2011. Binary regulation of Hippo pathway by Merlin/NF2, Kibra, Lgl, and Melted specifies and maintains postmitotic neuronal fate. *Dev Cell.* 21:874–887.

Kremerskothen J, Plaas C, Buther K, Finger I, Veltel S, Matanis T, Liedtke T, Barnekow A. 2003. Characterization of KIBRA, a novel WW domain-containing protein. *Biochem Biophys Res Commun.* 300: 862–867.

Makuch L, Volk L, Anggono V, Johnson RC, Yu Y, Duning K, Kremerskothen J, Xia J, Takamiya K, Huganir RL. 2011. Regulation of AMPA receptor function by the human memory-associated gene KIBRA. *Neuron* 71:1022–1029.

Meerbrey KL, Hu G, Kessler JD, Roarty K, Li MZ, Fang JE, Herschkowitz JI, Burrows AE, Ciccia A, Sun T, et al. 2011. The pINDUCER lentiviral toolkit for inducible RNA interference in vitro and in vivo. *Proc Natl Acad Sci U S A.* 108:3665–3670.

Mosmann T. 1983. Rapid colorimetric assay for cellular growth and survival: application to proliferation and cytotoxicity assays. *J Immunol Methods.* 65:55–63.

Nguyen DK, Yang F, Kaul R, Alkan C, Antonellis A, Friery KF, Zhu B, de Jong PJ, Disteche CM. 2011. Clcn4-2 genomic structure differs between the X locus in *Mus spretus* and the autosomal locus in *Mus musculus*: AT motif enrichment on the X. *Genome Res.* 21: 402–409.

Poernbacher I, Baumgartner R, Marada SK, Edwards K, Stocker H. 2012. *Drosophila* Pez acts in Hippo signaling to restrict intestinal stem cell proliferation. *Curr Biol.* 22:389–396.

Robinson-Rechavi M, Huchon D. 2000. RRTree: relative-rate tests between groups of sequences on a phylogenetic tree. *Bioinformatics* 16: 296–297.

Rosse C, Formstecher E, Boeckeler K, Zhao Y, Kremerskothen J, White MD, Camonis JH, Parker PJ. 2009. An aPKC-exocyst complex controls paxillin phosphorylation and migration through localised JNK1 activation. *PLoS Biol.* 7:e1000235.

Schneider A, Huentelman MJ, Kremerskothen J, Duning K, Spoelgen R, Nikolich K. 2010. KIBRA: a new gateway to learning and memory? *Front Aging Neurosci.* 2:4.

Schulze U, Vollenbroeker B, Braun DA, Le TV, Granado D, Kremerskothen J, Fraenzel B, Klosowski R, Barth J, Fufezan C, et al. 2014. The Vac14-interaction network is linked to regulators of the endolysosomal and autophagic pathway. *Mol Cell Proteomics* 13(6):1397–1411.

Sen A, Nagy-Zsver-Vadas Z, Krahn MP. 2012. *Drosophila* PATJ supports adherens junction stability by modulating Myosin light chain activity. *J Cell Biol.* 199:685–698.

Shorning BY, Clarke AR. 2011. LKB1 loss of function studied in vivo. *FEBS Lett.* 585:958–966.

Stein PL, Vogel H, Soriano P. 1994. Combined deficiencies of Src, Fyn, and Yes tyrosine kinases in mutant mice. *Genes Dev.* 8: 1999–2007.

Talavera G, Castresana J. 2007. Improvement of phylogenies after removing divergent and ambiguously aligned blocks from protein sequence alignments. *Syst Biol.* 56:564–577.

Tamura K, Peterson D, Peterson N, Stecher G, Nei M, Kumar S. 2011. MEGA5: molecular evolutionary genetics analysis using maximum likelihood, evolutionary distance, and maximum parsimony methods. *Mol Biol Evol.* 28:2731–2739.

Traer CJ, Rutherford AC, Palmer KJ, Wassmer T, Oakley J, Attar N, Carlton JG, Kremerskothen J, Stephens DJ, Cullen PJ. 2007. SNX4 coordinates endosomal sorting of TfnR with dynein-mediated transport into the endocytic recycling compartment. *Nat Cell Biol.* 9: 1370–1380.

Varelas X, Miller BW, Sopko R, Song S, Gregorieff A, Fellouse FA, Sakuma R, Pawson T, Hunziker W, McNeill H, et al. 2010. The Hippo pathway regulates Wnt/beta-catenin signaling. *Dev Cell.* 18:579–591.

Varelas X, Sakuma R, Samavarchi-Tehrani P, Peerani R, Rao BM, Dembowy J, Yaffe MB, Zandstra PW, Wrana JL. 2008. TAZ controls Smad nucleocytoplasmic shuttling and regulates human embryonic stem-cell self-renewal. *Nat Cell Biol.* 10:837–848.

Vogt-Eisele A, Krüger C, Duning K, Weber D, Spoelgen R, Pitzer C, Plaas C, Eisenhardt G, Meyer A, Vogt G, et al. 2014. KIBRA (KIdney/BRAin protein) regulates learning and memory and stabilizes Protein kinase Mζ. *J Neurochem.* 128:686–700.

Waterston RH, Lindblad-Toh K, Birney E, Rogers J, Abril JF, Agarwal P, Agarwala R, Ainscough R, Alexandersson M, An P, et al. and Mouse Genome Sequencing Consortium. 2002. Initial sequencing and comparative analysis of the mouse genome. *Nature* 420: 520–562.

Wehr MC, Laage R, Bolz U, Fischer TM, Grunewald S, Scheek S, Bach A, Nave KA, Rossner MJ. 2006. Monitoring regulated protein–protein interactions using split TEV. *Nat Methods.* 3:985–993.

Wilgenbusch JC, Swofford D. 2003. Inferring evolutionary trees with PAUP*. *Curr Protoc Bioinform.* Chapter 6:Unit 6.4.

Xiao L, Chen Y, Ji M, Dong J. 2011. KIBRA regulates Hippo signaling activity via interactions with large tumor suppressor kinases. *J Biol Chem.* 286:7788–7796.

Xiao L, Chen Y, Ji M, Volle DJ, Lewis RE, Tsai MY, Dong J. 2011. KIBRA protein phosphorylation is regulated by mitotic kinase aurora and protein phosphatase 1. *J Biol Chem.* 286:36304–36315.

Yang S, Ji M, Zhang L, Chen Y, Wennmann DO, Kremerskothen J, Dong J. 2014. Phosphorylation of KIBRA by the extracellular signal-regulated kinase (ERK)-ribosomal S6 kinase (RSK) cascade modulates cell proliferation and migration. *Cell Signal.* 26:343–351.

Yin M, Zhang L. 2011. Hippo signaling: a hub of growth control, tumor suppression and pluripotency maintenance. *J Genet Genomics.* 38: 471–481.

Yoshihama Y, Chida K, Ohno S. 2012. The KIBRA-aPKC connection: a potential regulator of membrane trafficking and cell polarity. *Commun Integr Biol.* 5:146–151.

Yoshihama Y, Izumisawa Y, Akimoto K, Satoh Y, Mizushima T, Satoh K, Chida K, Takagawa R, Akiyama H, Ichikawa Y, et al. 2013. High expression of KIBRA in low atypical protein kinase C-expressing gastric cancer correlates with lymphatic invasion and poor prognosis. *Cancer Sci.* 104:259–265.

Yoshihama Y, Sasaki K, Horikoshi Y, Suzuki A, Ohtsuka T, Hakuno F, Takahashi S, Ohno S, Chida K. 2011. KIBRA suppresses apical exocytosis through inhibition of aPKC kinase activity in epithelial cells. *Curr Biol.* 21:705–711.

Yu FX, Guan KL. 2013. The Hippo pathway: regulators and regulations. *Genes Dev.* 27:355–371.

Yu FX, Mo JS, Guan KL. 2012. Upstream regulators of the Hippo pathway. *Cell Cycle* 11:4097–4098.

Yu FX, Zhao B, Panupinthu N, Jewell JL, Lian I, Wang LH, Zhao J, Yuan H, Tumaneng K, Li H, et al. 2012. Regulation of the Hippo-YAP pathway by G-protein-coupled receptor signaling. *Cell* 150:780–791.

Yu J, Zheng Y, Dong J, Klusza S, Deng WM, Pan D. 2010. Kibra functions as a tumor suppressor protein that regulates Hippo signaling in conjunction with Merlin and Expanded. *Dev Cell.* 18:288–299.

Zhang J. 2012. Genetic redundancies and their evolutionary maintenance. *Adv Exp Med Biol.* 751:279–300.

Zhang Y, Castillo-Morales AC, Jiang M, Zhu Y, Hu L, Urrutia AO, Kong X, Hurst LD. 2013. Genes that escape X-inactivation in humans have high intraspecific variability in expression, are associated with mental impairment but are not slow evolving. *Mol Biol Evol.* 30:2588–25601.

Zhao B, Kim J, Ye X, Lai ZC, Guan KL. 2009. Both TEAD-binding and WW domains are required for the growth stimulation and oncogenic transformation activity of yes-associated protein. *Cancer Res.* 69:1089–1098.

Zhao B, Li L, Tumaneng K, Wang CY, Guan KL. 2010. A coordinated phosphorylation by Lats and CK1 regulates YAP stability through SCF (beta-TRCP). *Genes Dev.* 24:72–85.

Zhao B, Tumaneng K, Guan KL. 2011. The Hippo pathway in organ size control, tissue regeneration and stem cell self-renewal. *Nat Cell Biol.* 13:877–883.

Zhu H, Zhou Z, Wang D, Liu W, Zhu H. 2013. Hippo pathway genes developed varied exon numbers and coevolved functional domains in metazoans for species specific growth control. *BMC Evol Biol.* 13:76.